Progress In Electromagnetics Research, Vol. 155, 27–38, 2016

Synthesis of Sparse or Thinned Linear and Planar Arrays Generating Reconfigurable Multiple Real Patterns by Iterative Linear Programming

Yanhui Liu[1], Pengfei You[1], Chunhui Zhu[1, *], Xiaofeng Tan[2], and Qing Huo Liu[3]

Abstract—It is shown in this paper that the problem of reducing the number of elements for multiple-pattern arrays can be solved by a sequence of reweighted ℓ_1 optimizations under multiple linear constraints. To do so, conjugate symmetric excitations are assumed so that the upper and lower bounds for each pattern can be formulated as linear inequality constraints. In addition, we introduce an auxiliary variable for each element to define the common upper bound of both the real and imaginary parts of multiple excitations for different patterns, so that only linear inequality constraints are required. The objective function minimizes the reweighted ℓ_1-norm of these auxiliary variables for all elements. Thus, the proposed method can be efficiently implemented by the iterative linear programming. For multiple desired patterns, the proposed method can select the common elements with multiple set of optimized amplitudes and phases, consequently reducing the number of elements. The radiation characteristics for each pattern, such as the mainlobe shape, response ripple, sidelobe level and nulling region, can be accurately controlled. Several synthesis examples for linear array, rectangular/triangular-grid and randomly spaced planar arrays are presented to validate the effectiveness of the proposed method in the reduction of the number of elements.

1. INTRODUCTION

Reconfigurable arrays can radiate dual or more patterns by varying only element excitations, and consequently reduce the number of antennas and the cost of the whole hardware system. These arrays have been widely used in applications, such as multi-functional radars and communication systems [1]. Many practical methods have been introduced in the past to produce a reconfigurable aperture with multiple patterns, including multi-mode feeding technologies for reflector antennas [2], and some multi-beam forming networks for antenna arrays [3–6]. Other studies focus on the design of phase-differentiated antenna arrays using some sophisticated synthesis methods, such as alternating projection approaches [7, 8], stochastic optimization algorithms [9–11], and some other techniques [12, 13]. The phase-differentiated antenna array reported in the literature usually adopts a uniform spacing and the common excitation amplitude distribution for multiple patterns. In such a way, the complexity of designing a feeding network is greatly reduced. On the other hand, advanced techniques such as the digital beamforming hardware have increasingly been developed in recent years [14]. These techniques allow for much more flexibility in both the design of array's geometry and the individual control of excitation amplitudes and phases. From the perspective of pattern synthesis, relaxing the both limitations of uniform spacing and the common amplitude distribution would provide much more degrees of freedom to achieve the synthesis performance improvement, such as the reduction in the number of elements [15].

Received 4 December 2015, Accepted 10 February 2016, Scheduled 17 February 2016
* Corresponding author: Chunhui Zhu (zhuchhxd@xmu.edu.cn).
[1] Department of Electronic Science, Xiamen University, Xiamen, Fujian 361005, China. [2] Overseas Education College, Jimei University, Xiamen, Fujian 361021, China. [3] Department of Electrical and Computer Engineering, Duke University, Durham, NC 27708, USA.

This work focuses on the synthesis of reconfigurable multiple patterns with fewer elements by selecting the common ones with optimized excitation amplitudes and phases. Some synthesis methods by using nonuniform element positions [16–22], or by applying thinning techniques [23–25], have been presented to effectively reduce the number of elements. However, these reviewed techniques are proposed for the synthesis of single-pattern arrays. It is unclear whether they can be easily extended to the multiple-pattern case since the best element positions usually change with different patterns. Some stochastic optimization algorithms capable of finding the global optimal solutions, such as in [26–29], may be appropriate, but they can be time-consuming since many unknowns including positions, multiple sets of excitations and even the number of elements, need to be determined. Recently, the extended forward-backward matrix pencil method (FBMPM) has been applied to find the common element positions with optimized excitations for multiple desired patterns [15]. This method is indeed effective for reducing the number of elements. However, the extended FBMPM deals only with the case of linear arrays, and the extension to planar arrays is not available right now. Note that, to the best of our knowledge, the problem of reducing the number of elements for a planar array with multiple patterns has been never discussed in the literature.

Here we will show that the synthesis problem mentioned above can be formulated into a sequence of reweighted ℓ_1-norm optimizations under multiple linear constraints. The iterative reweighted ℓ_1 optimization was presented in [30], and recently this idea was used to reduce the number of elements for a single focused beam or shaped pattern, by developing the iterative second-order cone programming (SOCP) in [31–33] or sequential compressive sensing (CS) approach in [34]. We now apply this idea to reduce the number of elements for multiple-pattern arrays by selecting the best common elements, each with multiple optimized excitations, under multiple power pattern requirements that are all given by upper and lower bounds. However, the lower bound used for a shaped power pattern is in general non-convex [31]. To overcome this problem, the excitation distribution is assumed to be conjugate-symmetrical for each pattern. In this case, both the upper and lower pattern bounds can be transformed into the form of linear inequalities. Although this assumption cannot exploit the maximum degrees of synthesis freedom [35], it effectively eliminates the non-convexity of the lower bound. Note that this assumption does not really reduce the solution space for a class of patterns which would have conjugate-symmetrical excitations (e.g., some of pencil-beam patterns). In addition, the choice of a symmetrical layout and symmetrical amplitudes can greatly simplify the beamforming network. Hence, this choice has been widely adopted by many single-pattern synthesis methods, for example, in [23] and [31]. To cast the problem of finding the common element positions for multiple patterns into the form of linear programming, we introduce an auxiliary variable to define the common upper bound of the real and imaginary parts of multiple excitations for each element. Consequently, multiple linear inequalities (other than the second-order cone constraints) can be used to deal with the complex excitations in the framework of ℓ_1 optimization. Hence, the proposed method can be very efficiently implemented by iteratively performing the linear programming (LP) that is more computationally efficient than the iterative SOCP. This method can be applicable to the synthesis of an arbitrary array geometry with multiple pattern requirements (with the only limitation of conjugate-symmetrical excitations), and can be considered as a significant extension of the method presented in [31] where the problem of synthesizing the rectangular-grid array with a single shaped pattern has been successfully dealt.

To validate the effectiveness and advantages of the proposed method, several examples are given for synthesizing multiple patterns for linear array, rectangular/triangular-grid arrays, and randomly spaced planar array. Significant savings in the number of elements are achieved in the tested examples.

2. FORMULATION AND ALGORITHMS

2.1. Conjugate-Symmetrical Array Model

Consider a reconfigurable array of N elements that can radiate multiple desired patterns by varying the element excitation distributions. The kth array's pattern (for $k = 1, 2, \ldots, K$) is given by

$$F_k(\theta, \phi) = \sum_{n=1}^{N} w_{n,k} e^{-j\beta \mathbf{r}_n^T e(\theta,\phi)} \tag{1}$$

where $j = \sqrt{-1}$, $\beta = 2\pi/\lambda$, $\mathbf{r}_n = [x_n, y_n]^T \in \Re^2$ denotes the location of nth element, and $w_{n,k}$ denotes the complex excitation of the nth element for the kth pattern. $e(\theta, \phi) = [\sin\theta\cos\phi, \sin\theta\sin\phi]^T$ is the unit direction vector. For different patterns, the array element has the common position but with probably different excitations.

Assume that the element excitations of this array are conjugate-symmetrical. For an even N, we have $\mathbf{r}_n = -\mathbf{r}_{N+1-n}$ and $(w_{n,k})^* = w_{N+1-n,k}$ for $n = 1, 2 \ldots, N/2$. With this constraint, it can be easily proven that the pattern $F_k(\theta, \phi)$ is real-valued, and can be expressed as

$$F_k(\theta, \phi) = 2\mathrm{Re}\left\{\sum_{n=1}^{N/2} w_{n,k} e^{-j\beta\mathbf{r}_n^T e(\theta,\phi)}\right\} \tag{2}$$

Note that the above formula can be also applicable to the array with an odd N, only if we treat it with $\mathbf{r}_{N/2} = \mathbf{r}_{N/2+1} = 0$ and $w_{N/2,k} = w_{N/2+1,k} \in \Re$. By defining the vectors

$$\mathbf{a}(\theta, \phi) = \left[e^{-j\beta\mathbf{r}_1^T e(\theta,\phi)}, e^{-j\beta\mathbf{r}_2^T e(\theta,\phi)}, \ldots, e^{-j\beta\mathbf{r}_{N/2}^T e(\theta,\phi)}\right]^T \tag{3}$$

$$\mathbf{W}_k = \left[w_{1,k}, w_{2,k}, \ldots, w_{N/2,k}\right]^T \tag{4}$$

and

$$\mathbf{s}^T(\theta, \phi) = \left[2\mathrm{Re}\left\{\mathbf{a}^T(\theta, \phi)\right\}, -2\mathrm{Im}\left\{\mathbf{a}^T(\theta, \phi)\right\}\right] \tag{5}$$

$$\mathbf{z}_k^T = \left[\mathrm{Re}\left\{W_k^T\right\}, \mathrm{Im}\left\{W_k^T\right\}\right] \tag{6}$$

we can rewrite Eq. (2) as

$$F_k(\theta, \phi) = \mathbf{s}^T(\theta, \phi)\,\mathbf{z}_k \tag{7}$$

Since $F_k(\theta, \phi)$ is real-valued, we have

$$|F_k(\theta, \phi)| = \begin{cases} \mathbf{s}^T(\theta, \phi)\,\mathbf{z}_k, & \text{for } F_k(\theta, \phi) \geq 0 \\ -\mathbf{s}^T(\theta, \phi)\,\mathbf{z}_k, & \text{for } F_k(\theta, \phi) < 0 \end{cases} \tag{8}$$

Note that the above array model can be considered as a more general version of the formulation in [31] which is derived for the case of rectangular-grid arrays.

2.2. Multiple-Pattern Constraints

The whole angle space can be subdivided into mainlobe region Ω^{ML} and sidelobe region Ω^{SL}. If a focused beam is desired, the look direction $(\theta^{\text{Look}}, \phi^{\text{Look}})$ should be specified. Assume that we have P focused beams and Q shaped patterns ($K = P + Q$). Each pattern can be produced by one individual set of excitations, but they share with the common element positions. The multiple patterns can be formulated as the following constraints.

1) Focused Beams $(p = 1, 2, \ldots, P)$

$$\begin{cases} \mathbf{s}^T\left(\theta_p^{\text{Look}}, \phi_p^{\text{Look}}\right)\mathbf{z}_p = 1 \\ -U_p(\theta, \phi) \leq \mathbf{s}^T(\theta, \phi)\,\mathbf{z}_p \leq U_p(\theta, \phi), \quad \text{for } (\theta, \phi) \in \Omega_p^{SL} \end{cases} \tag{9}$$

2) Shaped Patterns $(q = P + 1, P + 2, \ldots, K)$

$$\begin{cases} L_q(\theta, \phi) \leq \mathbf{s}^T(\theta, \phi)\,\mathbf{z}_q \leq U_q(\theta, \phi), & \text{for } (\theta, \phi) \in \Omega_q^{ML} \\ -U_q(\theta, \phi) \leq \mathbf{s}^T(\theta, \phi)\,\mathbf{z}_q \leq U_q(\theta, \phi), & \text{for } (\theta, \phi) \in \Omega_q^{SL} \end{cases} \tag{10}$$

In the above, $U_p(\theta, \phi)$ or $U_q(\theta, \phi)$ denotes the upper bound of the pth or qth amplitude pattern which is a (θ, ϕ)-dependent function. By presetting an appropriate upper bound, one can obtain an arbitrary sidelobe distribution including pattern nulls if required. $L_q(\theta, \phi)$ denotes the lower bound of the qth shaped amplitude pattern. Note that Eqs. (9) and (10) have modified the formulation of Eqs. (9c) and (9d) in [31] for the sidelobe region since $\mathbf{s}^T(\theta, \phi)\mathbf{z}_q$ may be negative. Besides, the best element positions usually vary with different patterns. So, the difficulty comes from determining the best common element positions with as few elements as possible to simultaneously satisfy the multiple pattern constraints.

2.3. Element Selection Using Iterative Reweighted ℓ_1 Optimization

The above constraints describe the feasible solution space where every solution meets the desired multiple pattern requirements. Among all the feasible solutions, the one with fewer non-zero excitations is preferred. The problem of finding the best common elements for a sparse solution can be formulated as

$$\min_{z_1,\ldots,z_k} \|t\|_0, \text{ under } Const. \text{ (9) and (10)} \tag{11}$$

where t is defined as

$$Const. \begin{cases} t = [t_1, t_2, \ldots, t_{N/2}]^T \\ t_n \geq |w_{n,k}|, \text{ for any } k \end{cases} \tag{12}$$

In the above, $\|t\|_0$ is a ℓ_0-norm that represents the number of non-zero elements in the vector t (ℓ_0-norm is not strictly speaking a norm since it is not homogeneous, but it has been widely used in compressive sensing and other areas), and t_n is defined as the common magnitude bound of the multiple excitations for different patterns at the nth element. Eq. (12) can be described by multiple second-order cone (SOC) constraints. However, due to the non-convex objective, Eq. (11) is a combinatorial optimization problem that usually costs huge CPU time. A practical alternative can be obtained by replacing the ℓ_0-norm with ℓ_1-norm optimization and changing the definition of t_n, which is given by

$$\min_{z_1,\ldots,z_k} \sum_{n=1}^{N/2} t_n \text{ under } Const. \text{ (9) and (10)}, \tag{13}$$

and

$$Const. \begin{cases} t = [t_1, t_2, \ldots, t_{N/2}]^T \\ t_n \geq |\mathrm{Re}[w_{n,k}]|, \text{ for any } k \\ t_n \geq |\mathrm{Im}[w_{n,k}]|, \text{ for any } k \end{cases} \tag{14}$$

Now, problem in Eq. (13) can be efficiently solved by the linear programming.

The ℓ_1-norm has been extensively used in many applications to produce the sparse solution. However, there also exists a significant difference between ℓ_0 and ℓ_1 norms. That is, larger coefficients are penalized more heavily than smaller coefficients in the ℓ_1 norm. Recently, the iterative reweighted ℓ_1-norm optimization was presented in [30] to approach as closely as possible to ℓ_0-norm for enhanced sparsity. This method has been successfully applied to the sensors selection for single-pattern arrays in [31–33]. Now, we extend the idea to enhance the sparsity of the multiple-pattern array synthesis. The weighted ℓ_1 optimization at the kth iteration is given by

$$\min_{z_1,\ldots,z_k} \sum_{n=1}^{N/2} \alpha_n^l t_n \text{ under } Const. \text{ (9), (10) and (14)}, \tag{15}$$

where $\alpha_n^l = 1/(t_n^{l-1} + \delta)$ for $l > 1$, and t_n^{l-1} is the result obtained from the $(l-1)$th iteration. The parameter $\delta > 0$ is used to provide numerical stability when $t_n^{l-1} = 0$. Usually, δ is set to be slightly larger than the smallest excitation coefficient [31]. Larger weight α_n^l is obtained for a smaller coefficient, which penalizes the smaller coefficient more approaching to zero at the next iteration. In the initial iteration ($l = 1$), we set $\alpha_n = 1$, and the problem in Eq. (15) reduces to the original ℓ_1 optimization of Eq. (13). The solutions of $z_1, z_2, \ldots, z_K$ are updated by the iteration procedure until l attains a specified maximum iteration number, or the number of selected elements maintains the same after multiple iterations.

Note that the whole optimization process in Eq. (15) needs to sequentially perform the linear programming solver, but all the matrices and vectors defined above are fixed at each iteration except that the vector $\mathbf{b}$ needs to be updated at each iteration. Many optimization toolboxes are available to solve the linear programming problem, such as the MATLAB function 'linprog' and the SeDuMi (Self-Dual-Minimization) tool [36].

3. NUMERICAL RESULTS

To validate the effectiveness of the proposed method, we provide several synthesis examples with different situations including linear arrays, rectangular/triangular-grid and randomly spaced planar arrays. In these examples, we set the parameter $\delta = \delta_0 * \max\{t_n^0\}$ fixed in the iteration procedure, where t_n^0 $(n = 0, 1, \ldots, N-1)$ are obtained from the first iteration. How to choose the value of δ_0 will be shown in the following examples. For all the tested cases, we set the maximum number of iterations to be 15. However, the synthesis procedure can be stopped if the number of selected elements maintains the same for three iterations. The excitation with very small t_n (e.g., $t_n \le \max\{t_n\}/10^5$) are discarded. The comparisons with some other methods are also given in these examples.

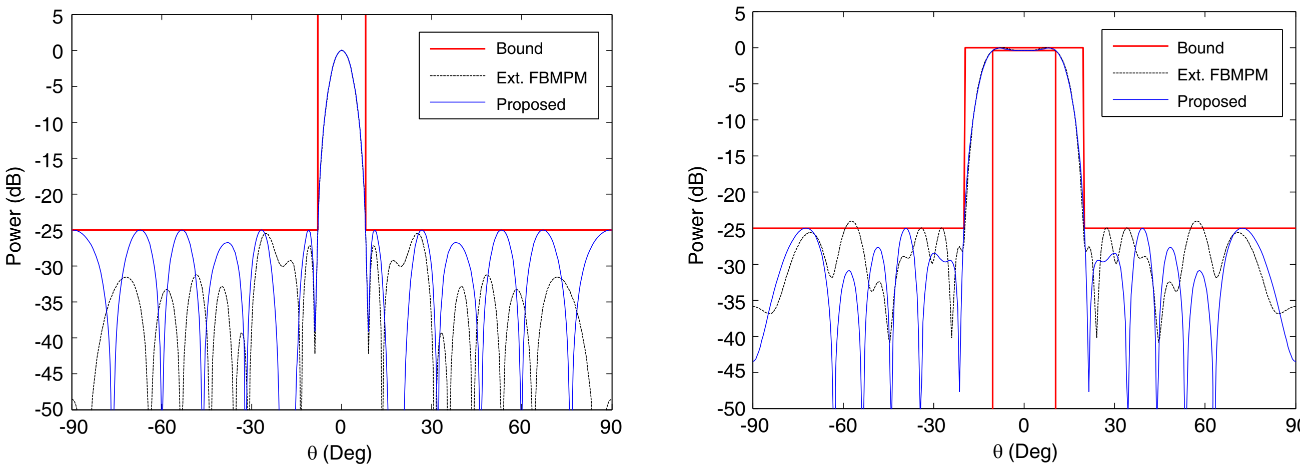

(a) (b)

Figure 1. The dual patterns synthesized by the proposed method with 14 elements, and the reconstructed patterns by the extended FBMPM with 15 elements in [15]: (a) focused beam, and (b) flat-top pattern.

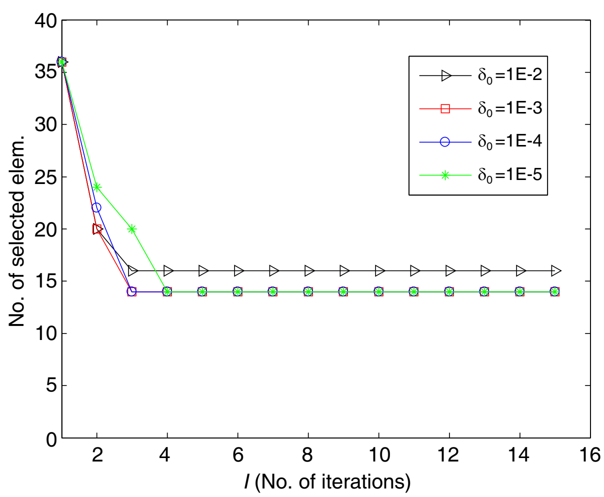

Figure 2. The number of selected elements versus the iteration number l for different choices of δ_0.

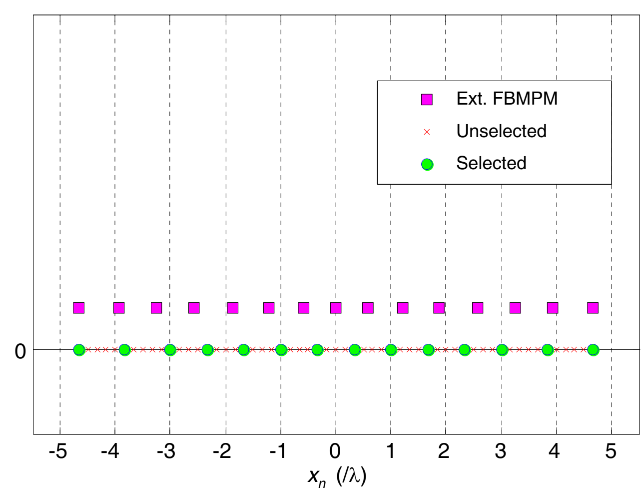

Figure 3. The selected and unselected element positions for the synthesized dual patterns in Fig. 1, and the positions obtained by the extended FBMPM in [15].

3.1. Linear Array

As the first example, we consider a dual-pattern including a pencil beam and a flat-top beam, which was obtained by the extended forward-backward matrix pencil method (FBMPM) using 15 nonuniformly spaced elements [15]. Now, to apply the proposed method, we put 57 potential element positions with spacing of $\lambda/6$. Appropriate upper and lower bounds are used for the desired pattern characteristics for each pattern, as shown in Fig. 1. In the iteration, we set the parameter $\delta = \delta_0 * \max\{t_n^0\}$ with varying $\delta_0 = [10^{-2}, 10^{-3}, 10^{-4}, 10^{-5}]$ to check its effect on the performance of proposed method. Fig. 2 shows the number of selected elements versus the iteration number for different choices of δ_0. As can be seen, $\delta_0 = 10^{-3}$ or 10^{-4} would be a good choice. With this choice, the proposed method takes only 3 iterations to reach the convergence, and only 14 elements are finally selected. Note that in the first iteration, we actually solve problem (13), the unweighted ℓ_1 optimization, which gives 36 selected elements. Clearly, the later weighted ℓ_1-norm optimizations is very effective to further reduce the number of selected elements. The synthesized focused and shaped patterns are shown in Figs. 1(a) and (b), respectively. For comparison, the patterns obtained by the extended FBMPM in [12] are also shown here. As can be seen, the dual patterns synthesized by the proposed method strictly meet their specified upper and lower bounds, and has more accurate sidelobe control than the extended FBMPM. Fig. 3 shows the selected element positions and those given by the extended FBMPM. We can see that the proposed method saved one more element than the extended FBMPM. If compared with a uniformly spaced array by using 20 elements to occupy the same aperture, the saving in the number of elements is 30%. Fig. 4 shows the excitation distributions of the synthesized focused and shaped patterns by the proposed method. Due to the symmetry property of the dual patterns, their excitation distributions are also symmetrical.

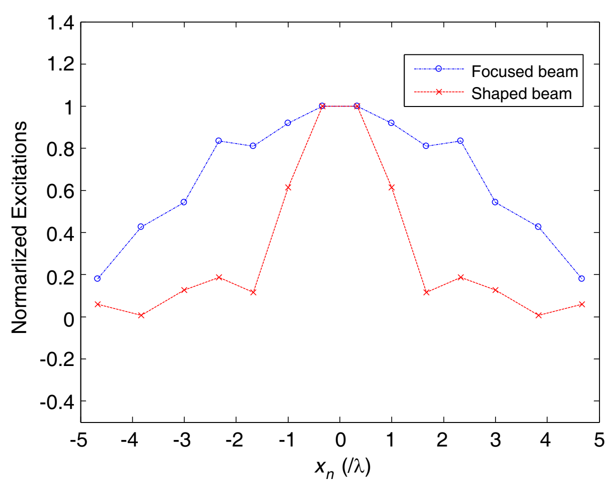

Figure 4. The normalized excitation distributions for the synthesized dual patterns in Fig. 1.

3.2. Rectangular-Grid Planar Array

In the second example, we consider to synthesize a planar array with dual patterns. For the first pattern, the mainlobe is specified as circular-shaped region $\{(u, v) : |u^2 + v^2 \leq 0.2^2\}$ with a ripple ≤ 1 dB, where $u = \sin\theta\cos\phi$ and $v = \sin\theta\sin\phi$. The sidelobe region is defined as $\{(u, v) : |u^2 + v^2 \geq 0.4^2\}$ with the sidelobe level (SLL) ≤ -25.85 dB. This pattern was synthesized by the iterative second-order cone programming (SOCP) in [31] where 85 antennas were finally selected from a 11×11 rectangular-grid planar array with a spacing of $\lambda/2$. For the second pattern, the mainlobe is defined as a diamond-shaped region $\{(u, v) : ||u - 0.2| + |v - 0.2| \leq 0.2\}$ with a ripple ≤ 1 dB, and the sidelobe level is SLL ≤ -24.30 dB for the region $\{(u, v) : ||u - 0.2| + |v - 0.2| \geq 0.4\}$. A circular-shaped null region $\{(u, v) : |(u - 0.5)^2 + (v - 0.5)^2 \leq 0.1^2\}$ with SLL ≤ -50 dB is also added into the second pattern. The second pattern was also synthesized in [31] with a 14×14 array with spacing of $\lambda/2$. Since no

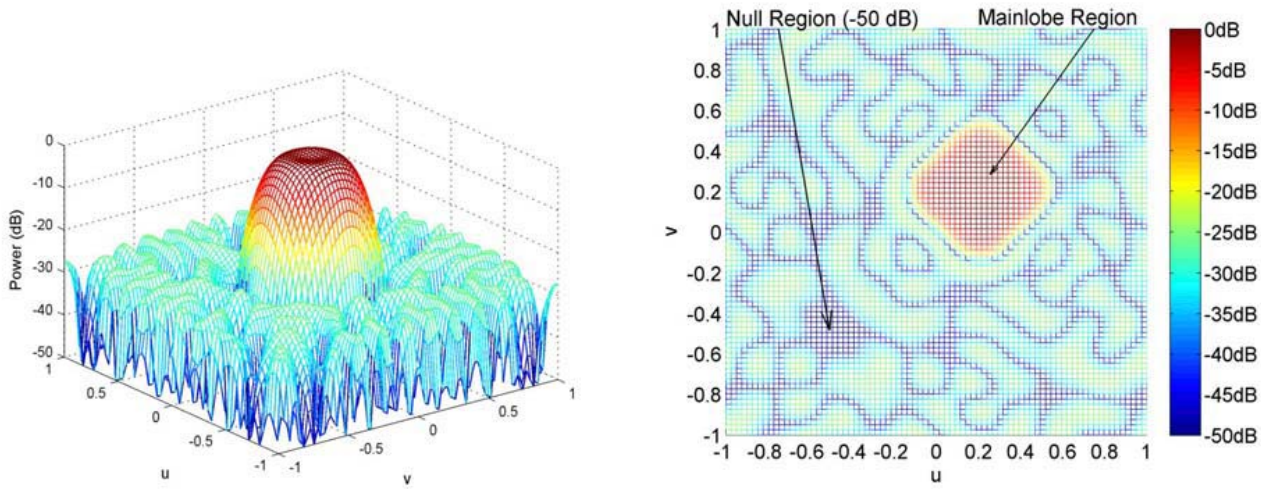

(a) (b)

Figure 5. The synthesized dual patterns by using 150 elements: (a) the circular-shaped pattern, and (b) the diamond-shaped pattern with a $-50\,\mathrm{dB}$ circular-shaped null region.

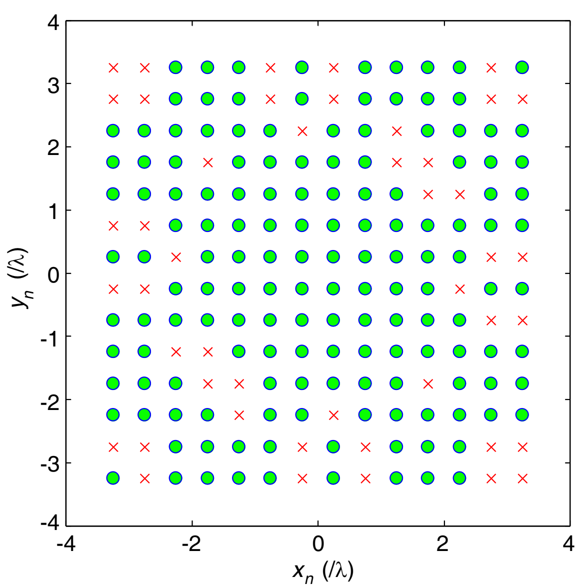

Figure 6. The selected ('∘') and unselected ('×') element positions for the rectangular gird array with dual patterns.

antenna selection is used for this pattern in [31], all the elements of this array are fully excited. We now use the proposed method to simultaneously synthesize the dual patterns by using only a single array. To compare with the results in [31], the initial array is used as the one with $\lambda/2$-spacing 14×14 elements. The parameter $\delta_0 = 10^{-4}$ is used in this example and the followings. 8 iterations are required for the proposed method to reach the convergence. Finally, 150 antennas are selected from the initial array for the dual patterns. The synthesized first and second patterns are shown in Figs. 5(a) and (b), respectively. The dual patterns in Fig. 5 strictly meet their specifications. The distribution of selected elements is shown in Fig. 6. Compared with the original 14×14 array with a single pattern, we have produced dual mainlobe-shaped patterns, and in addition we have saved 23.47% elements.

3.3. Triangular-Grid Planar Array

The proposed method can be applied to an arbitrary array with conjugate-symmetrical excitations. As the third example, we consider to synthesize a triangular-grid array with four patterns which have different mainlobe shapes. They are specified as follow:

(1) *focused beam*: $u = v = 0$ for the look direction, and $\{(u, v) : |u^2 + v^2 \geq 0.17^2\}$ for the sidelobe region;

(2) circular-shaped pattern: $\{(u, v) : |u^2 + v^2 \leq 0.2^2\}$ for the mainlobe region, and $\{(u, v) : |u^2 + v^2 \geq 0.4^2\}$ for the sidelobe region;

(3) *moon-like pattern*: $\{(u, v) : |(u + 0.35)^2 + v^2 \geq 0.5^2 \,\&\, u^2 + v^2 \leq 0.35^2\}$ for the mainlobe region, and the outside of $\{(u, v) : |(u + 0.5)^2 + v^2 \geq 0.5^2 \,\&\, u^2 + v^2 \leq 0.5^2\}$ for the sidelobe region;

(4) *rectangular-shaped pattern*: $\{(u, v) : ||u| \leq 0.25 \,\&\, |v| \leq 0.1\}$ for the mainlobe region, and the outside of $\{(u, v) : ||u| \leq 0.4 \,\&\, |v| \leq 0.2\}$ for the sidelobe region.

Note that the response ripple ≤ 1 dB and SLL ≤ -20 are used for all the patterns in this example. 247 potential element positions are used with the spacings of $d_y = \lambda/2$ and $d_x = \lambda/\sqrt{3}$. The proposed method takes 9 iterations to reach the convergence. The synthesized four patterns are shown in Figs. 7(a)–(d), respectively. It can be seen that for all these patterns, the mainlobe shapes are obtained as expected, and their sidelobe levels also meet the specifications. The distribution of selected antennas is shown in Fig. 8. Only 121 antennas are selected. So, we have reduced 51.01% elements from the array of all potential antennas. Note that in practice, we may not know exactly how many elements

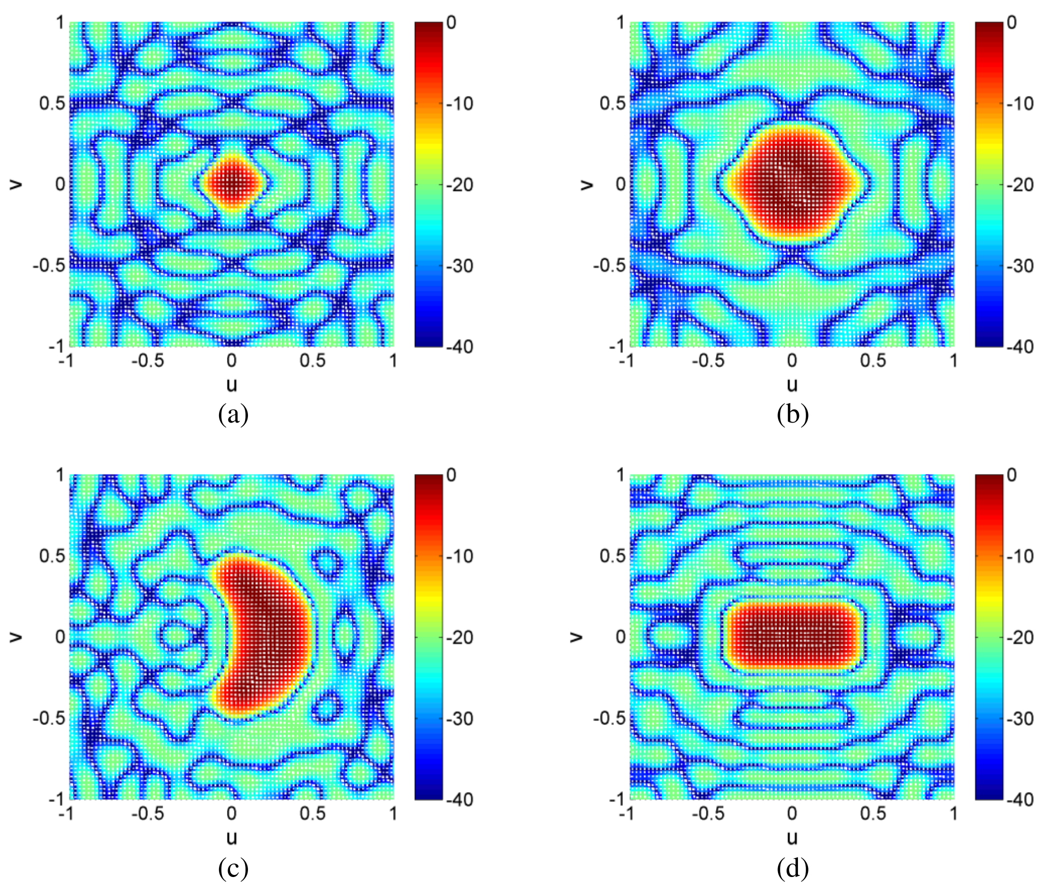

Figure 7. The synthesized four patterns by using 121 elements: (a) focused beam, (b) circular-shaped pattern, (c) moon-like pattern, and (d) rectangular-shaped pattern.

are required for multiple desired patterns, but we can assume a potential distribution with a relatively large number of elements and then apply the proposed method to select the appropriate antennas.

3.4. Randomly Spaced Planar Array

The last example is given to check if the proposed method can reduce the number of elements for a planar array with randomly spaced but symmetrically distributed elements. This array consists of 974 potential elements, and the positions for half of them are randomly generated, as shown in Fig. 9. Assume that the following dual patterns are desired:

(1) *focused beam*: $u = v = 0$ for the look direction, and $\{(u, v) : |u^2 + v^2 \geq 0.25^2\}$ for the sidelobe region;

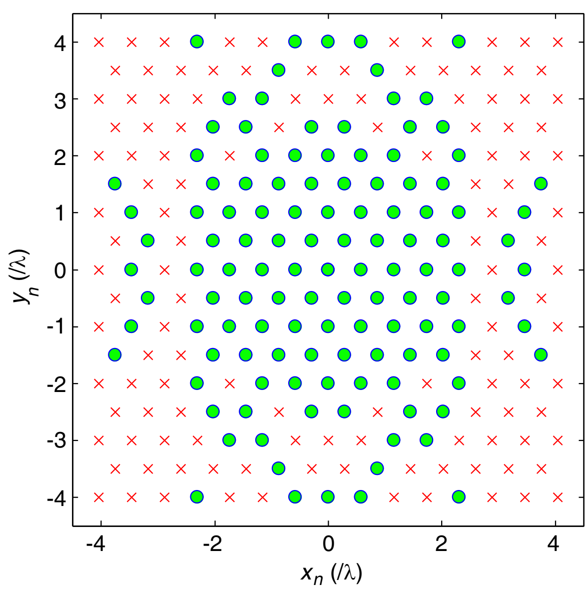

Figure 8. The selected ('○') and unselected ('×') element positions for the triangular grid array with four patterns.

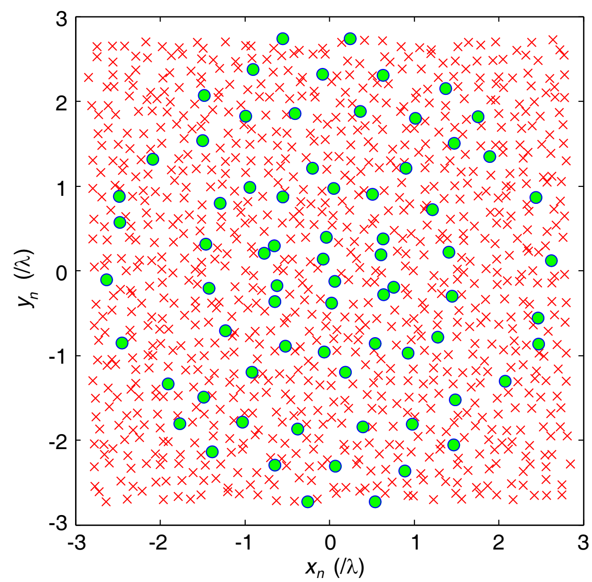

Figure 9. The selected ('○') and unselected ('×') element positions for the randomly spaced planar array with dual patterns.

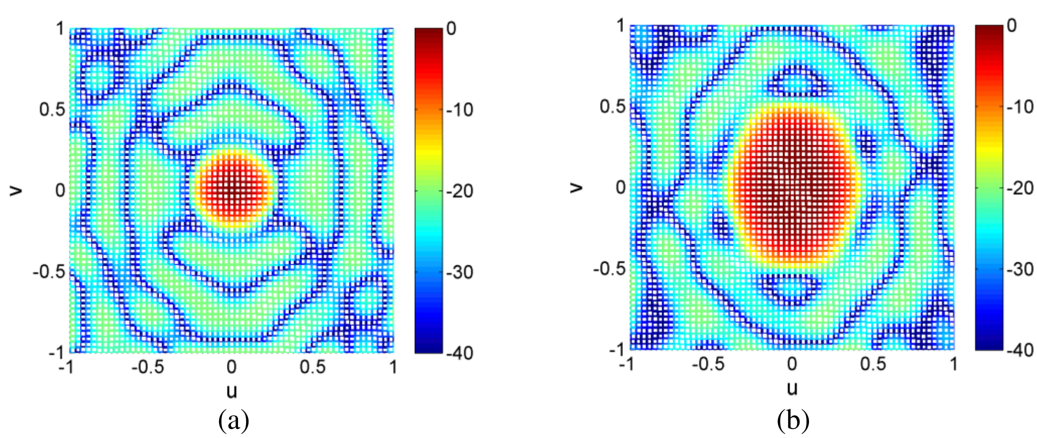

Figure 10. The synthesized dual patterns for the randomly spaced planar array by using 72 elements: (a) focused beam, and (b) elliptical-shaped pattern.

(2) *elliptical-shaped pattern*: $\{(u, v) : |u^2 + v^2/2 \leq 0.2^2\}$ for the mainlobe region, and $\{(u, v) : |u^2 + v^2/2 \geq 0.4^2\}$ for the sidelobe region.

The response ripple ≤ 1 dB and SLL ≤ -20 are still used for these dual patterns. The proposed iterative linear programming method is used to find the best common positions and the optimized excitations as well. 5 iterations are required to reach the convergence for this example. Finally, 72 elements are selected, as shown in Fig. 9. The synthesized focused and elliptical-shaped patterns are shown in Figs. 10(a) and (b), respectively. They completely meet their specifications again.

4. CONCLUSION

We have presented a new multiple-pattern synthesis method based on performing the iterative linear programming under multiple linear constraints. For multiple desired patterns, the proposed method can select the common antennas with multiple sets of optimized amplitudes and phases, each set corresponding to one pattern. Therefore, the number of elements required for multiple patterns can be significantly reduced. In addition, for each pattern, the characteristics such as the mainlobe shape, response ripple, sidelobe level and nulling region, can be easily controlled by specifying the upper and lower pattern bounds in the proposed method. A set of examples with different situations including linear array, rectangular/triangular-grid and randomly spaced planar arrays, have been tested to validate the effectiveness and advantages of this method. The comparisons with other synthesis methods in the literature are also included in these examples. The proposed method would be a preferred choice to reduce the number of elements or channels when multiple different far-field patterns are required in either electromagnetic or acoustic applications.

ACKNOWLEDGMENT

This work was supported by the National Natural Science Foundation of China (NSFC) under Grant Nos. 61301009, 41390453 and 61304110.

REFERENCES

1. Costantine, J., Y. Tawk, S. E. Barbin, and C. G. Christodoulou, "Reconfigurable antennas: Design and applications," *Proc. IEEE*, No. 3, 424–437, 2015.
2. Angeletti, P. and M. Lisi, "Multimode beamforming networks for space applications," *IEEE Antennas Propagat. Mag.*, Vol. 56, No. 1, 62–78, 2014.
3. Panduro, M. A. and C. del Río-Bocio, "Design of beam-forming networks for scannable multi-beam antenna arrays using CORPS," *Progress In Electromagnetics Research*, Vol. 84, 173–188, 2008.
4. Panduro, M. A. and C. del Río-Bocio, "Design of beam-forming networks using CORPS and evolutionary optimization," *International Journal of Electronics and Communications*, Vol. 63, No. 5, 353–365, 2009.
5. Arce, A., D. H. Covarrubias, M. A. Panduro, et al., "A new multiple-beam forming network design approach for a planar antenna array using CORPS," *Journal of Electromagnetic Waves and Applications*, Vol. 26, Nos. 2–3, 294–306, 2012.
6. Ferrando, N. and N. J. G. Fonseca, "Investigations on the efficiency of array fed coherently radiating periodic structure beam forming networks," *IEEE Trans. Antennas Propag.*, Vol. 59, No. 2, 493–502, 2011.
7. Bucci, O. M., G. Mazzarella, and G. Panariello, "Reconfigurable arrays by phase-only control," *IEEE Trans. Antennas Propag.*, Vol. 39, No. 7, 919–925, 1991.
8. Vescovo, R., "Reconfigurability and beam scanning with phase-only control for antenna arrays," *IEEE Trans. Antennas Propag.*, Vol. 56, No. 6, 1555–1565, 2008.
9. Gies, D. and Y. Rahmat-Samii, "Particle swarm optimization for reconfigurable phase-differentiated array design," *Microw. Opt. Technol. Lett.*, Vol. 38, No. 3, 168–175, 2003.

10. Mahanti, G. K., S. Das, and A. Chakraborty, "Design of phase-differentiated reconfigurable array antennas with minimum dynamic range ratio," *IEEE Antennas Wireless Propag. Lett.*, Vol. 5, No. 1, 262–264, 2006.
11. Akdagli, A., K. Guney, and B. Babayigit, "Clonal selection algorithm for design of reconfigurable antenna array with discrete phase shifters," *Journal of Electromagnetic Waves and Applications*, Vol. 21, No. 2, 215–227, 2007.
12. Morabito, A. F., A. Massa, P. Rocca, and T. Isernia, "An effective approach to the synthesis of phase only reconfigurable linear arrays," *IEEE Trans. Antennas Propag.*, Vol. 60, No. 8, 3622–3631, 2012.
13. Fuchs, B., "Application of convex relaxation to array synthesis problems," *IEEE Trans. Antennas Propag.*, Vol. 62, No. 2, 634–640, 2014.
14. Weedon, W. H., "Phased array digital beamforming hardware development at applied radar," *Proceedings of the IEEE Int. Symp. Phased Array Systems and Technology*, 854–859, Waltham, MA, Oct. 2010.
15. Liu, Y.-H., Q. H. Liu, and Z.-P. Nie, "Reducing the number of elements in multiple-pattern linear arrays by the extended matrix pencil methods," *IEEE Trans. Antennas Propag.*, Vol. 62, No. 2, 652–660, 2014.
16. Kumar, B. P. and G. R. Branner, "Design of unequally spaced arrays for performance improvement," *IEEE Trans. Antennas Propag.*, Vol. 47, No. 3, 511–523, 1999.
17. Murino, V., A. Trucco, and A. Tesei, "Beam pattern formulation and analysis for wide-band beamforming systems using sparse arrays," *Signal Process.*, Vol. 56, 177–183, 1997.
18. Liu, Y.-H., Z.-P. Nie, and Q. H. Liu, "Reducing the number of elements in a linear antenna array by the matrix pencil method," *IEEE Trans. Antennas Propag.*, Vol. 56, No. 9, 2955–2962, 2008.
19. Bucci, O. M., M. D'Urso, T. Isernia, et al., "Deterministic synthesis of uniform amplitude sparse arrays via new flexible density taper techniques," *IEEE Trans. Antennas Propag.*, Vol. 58, No. 6, 1949–1958, 2010.
20. Capozzoli, A., C. Curcio, A. Liseno, and G. Toso, "Phase-only synthesis of flat aperiodic reflectarrays," *Progress In Electromagnetics Research*, Vol. 133, 53–89, 2013.
21. Oliveri, G., M. Carlin, and A. Massa, "Complex-weight sparse linear array synthesis by Bayesian compressive sampling," *IEEE Trans. Antennas Propag.*, Vol. 60, No. 5, 2309–2326, 2012.
22. Oraizi, H. and M. Fallahpour, "Nonuniformly spaced linear array design for the specified beamwidth/sidelobe level or specified directivity/sidelobe level with coupling considerations," *Progress In Electromagnetics Research M*, Vol. 4, 185–209, 2008.
23. Holm, S., B. Elgetun, and G. Dahl, "Properties of the beam pattern of weight- and layout-optimized sparse arrays," *IEEE Trans. Ultrason., Ferroelect., Freq. Control.*, Vol. 44, No. 5, 983–991, 1997.
24. Zhang, W., L. Li, and F. Li, "Reducing the number of elements in linear and planar antenna arrays with sparseness constrained optimization," *IEEE Trans. Antennas Propag.*, Vol. 59, No. 8, 3106–3111, 2011.
25. Wang, X.-K., Y.-C. Jiao, and Y.-Y. Tan, "Gradual thinning synthesis for linear array based on iterative Fourier techniques," *Progress In Electromagnetics Research*, Vol. 123, 299–320, 2012.
26. Haupt, R. L., "Thinned array using genetic algorithms," *IEEE Trans. Antennas Propag.*, Vol. 42, No. 7, 993–999, 1994.
27. Liu, D., Q. Feng, W.-B. Wang, and X. Yu, "Synthesis of unequally spaced antenna arrays by using inheritance learning particle swarm optimization," *Progress In Electromagnetics Research*, Vol. 118, 205–221, 2011.
28. He, G. L. and B. Wu, "Unified particle swarm optimization with random ternary variables and its application to antenna array synthesis," *Journal of Electromagnetic Waves and Applications*, Vol. 28, No. 6, 752–764, 2014.
29. Chen, Y.-K, S.-W. Yang, and Z.-P. Nie, "The application of a modified differential evolution strategy to some array pattern synthesis problems," *IEEE Trans. Antennas Propag.*, Vol. 56, No. 7, 1919–1927, 2008.

30. Cands, E. J., M. B. Wakin, and S. P. Boyd, "Enhancing sparsity by reweighted l_1 minimization," *J. Fourier Analy. Appl.*, Vol. 14, 877–905, 2008.
31. Nai, S. E., W. Ser, Z. L. Yu, et al., "Beam pattern synthesis for linear and planar arrays with antenna selection by convex optimization," *IEEE Trans. Antennas Propag.*, Vol. 58, No. 12, 3923–3930, 2010.
32. Fuchs, B., "Synthesis of sparse arrays with focused or shaped beam pattern via sequential convex optimizations," *IEEE Trans. Antennas Propag.*, Vol. 60, No. 7, 3499–3503, 2012.
33. Prisco, G. and M. D'Urso, "Maximally sparse arrays via sequential convex optimizations," *IEEE Antennas Wireless Propag. Lett.*, Vol. 11, 192–195, 2012.
34. Zhao, X.-W., Q.-S. Yang, and Y.-H. Zhang, "Compressed sensing approach for pattern synthesis of maximally sparse non-uniform linear array," *IET Microw. Antennas Propag.*, Vol. 8, No. 5, 301–307, 2014.
35. Isernia, T., O. M. Bucci, and N. Fiorentino, "Shaped beam antenna synthesis problems: Feasibility criteria and new strategies," *Journal of Electromagnetic Waves and Applications*, Vol. 12, No. 1, 103–138, 1998.
36. Sturm, J. F., "Using SeDuMi 1.02, a MATLAB toolbox for optimization over symmetric cones," *Optimization Methods Software*, Vol. 11, No. 1–4, 625–653, 1999.